ISSN (Print) 1226-1750
ISSN (Online) 2233-6656
Journal of Magnetics 18(4), 422-427 (2013) http://dx.doi.org/10.4283/JMAG.2013.18.4.422

Effects of NEX on SNR and Artifacts in Parallel MR Images Acquired using Reference Scan

Yeong-Cheol Heo[1,2], Hae-Kag Lee[3], and Jae-Hwan Cho[2]*

[1]*Department of Radiology, Kyung Hee University Hospital at Gang-dong, Seoul 135-841, Korea*
[2]*Department of International Radiological Science, Hallym University of Graduate Studies, Seoul 135-841, Korea*
[3]*Department of Computer Science and Engineering, Soonchunhyang University, Asan 336-745 Korea*

(Received 12 August 2013, Received in final form 16 September 2013, Accepted 23 September 2013)

The aim of this study was to investigate effects of the number of acquisitions (NEX) on signal-to-noise (SNR) and artifacts in SENSE parallel imaging of magnetic resonance imaging (MRI). 3.0T MR System, 8 Channel sensitivity encoding (SENSE) head coils were used along with an *in-vivo* phantom. Reference sequence of 3D fast field echo (FFE) was consisted of NEX values of 2, 4, 6, 8, 10 and 12. The T2 turbo spin echo (TSE) sequence used for exams achieved SENSE factors of 1.2, 1.5, 1.8, 2.0, 2.2, 2.5, 2.8, 3.0, 3.2, 3.5, 3.8 and 4.0. Exams were conducted five times for each SENSE factor to measure signal intensity of the object, the posterior phase-encode direction and frequency direction. And SNR was calculated using mean values. SENSE artifacts were identified as background signal intensity in the phase-encoded direction using MRIcro. It was found that SNR increased but SENSE artifacts reduced with NEX of 4, 8 and 12 when the NEX increased in reference scan. It is therefore concluded that image quality can be improved with NEX of 4, 8 and 12 for reference scanning.

Keywords : reference scan, NEX, SNR, SENSE artifact

1. Introduction

The overall image acquisition time draws growing attention along with image contrast as MRI is commonly used as a diagnostic tool for patients with various medical conditions. Fast image acquisition is particularly embraced for images showing involuntary movements such as blood flow, cardiac motion and changes of brain activity. Among fast scanning techniques, k-space acceleration is basically used to increase image acquisition time. Other fast scanning methods include echo planar imaging (EPI), spiral scan imaging (SSI) and radiofrequency (RF) echo-based fast spin echo [1-4]. However, these techniques have limitations of producing only sequential images. Parallel imaging technique has emerged as new means of fast imagining that overcome the limitations of existing fast imaging techniques. Parallel imaging is designed to obtain images simultaneously using multiple receive coils. Once data is received by each coil, the typical imaging process for spatial encoding occur based on changes of gradients, but it is more parallel because spatial encoding simultaneously occurs utilizing sensitivity of each coil. In parallel imaging, MRI image is reconstructed using sensitivity information inherent in each coil and reducing the number of phase encoding steps. Simultaneous spatial encoding therefore shortens the image acquisition time. Accurate information on coil sensitivity map is required for accurate image reconstruction from sensitivity encoded data. A reference scan was therefore performed to obtain additional information on coil sensitivity before image reconstruction. While parallel imaging technology in MRI is useful to obtain images quickly, ghosting and blurring on reconstructed images, which are caused by involuntary movements of internal organs such as heart and cells and patient's movement pose limitation [10]. Many studies have addressed the limitation and suggested ways to improve image quality by detecting movements and adjusting them in advance. However, these studies used conventional MRI scans rather than parallel imaging techniques. Particularly no studies have ever used MRI reference scans. A reference scan can be used to reconstruct images from sensitivity encoded data and have a great impact on image quality. Generally, fixed NEX values are used for reference scans. However,

*Corresponding author: Tel: +82-70-8680-5900
Fax: +82-53-850-8244, e-mail: cho2404@hallym.ac.kr

changes in NEX values result in changes in image signals. It was therefore necessary to find how image quality is affected by changes in NEX values in reference scan. This study was aimed to investigate effects of NEX variations on signal-to-noise (SNR) and artifacts in SENSE parallel imaging of MRI.

2. Subjects and Methods

In this study, images were obtained using 3.0T MR System (Achieva Release 2.5, Philips, Netherlands), 8 channel SENSE head coils and phantom bottle assembly (contents 2.0 ± 0.05 g/L $CuSO_4 \cdot 5H_2O$, 4.5 ± 0.05 g/L NaCL, 1.89 L distilled water, P/N-102130), manufactured by *in-vivo* in Pewaukee, Wisconsin U.S.A 800-524-7476. In parallel imaging, sensitivity encoding reconstruction was performed using rectangular scans. Each fast reconstructed coil image for parallel imaging contains field of view (FOV) reduced by the reduction factor R. Each pixel I in coil images with reduced FOV is stacked with pixels ρ_k, ($k = 1, \ldots, R$) distributed at the same distance in full FOV image [12] Also, ρ_k pixels were weighted with the coil sensitivity S at the corresponding location in full FOV image. Therefore, the pixel $I_m = (x, y)$ obtained from m coil can be expressed as follows: [12]

$$I_m = (x, y) = S_m(x, y_1)\rho(x, y_1) + S_m(x, y_2)\rho(x, y_2) + \cdots + S_m(x, y_R)\rho(x, y_R) \quad (1)$$

Here m denotes the number of coils used and R denotes a reduction factor. The above formula can be expressed as follows [12]:

$$I_m = \Sigma_{n=1}^{R} S_{mn}\rho_n \quad (2)$$

And N linear equations can be constructed for m coils and R unknowns, and these equations can be expressed in the matrix form as follows: [12]

$$\vec{I} = \hat{S} \cdot \vec{\rho} \quad (3)$$

Vector $\vec{I}$ denotes complex image values for each coil. Thus vector $\vec{I}$ size is equal to the number of coils. The matrix S denotes sensitivity map for each coil at the corresponding positions of pixels superimposed with R pixels. $\hat{S}$ is an m × n. Vector $\vec{\rho}$ denotes a set of pixels in the full FOV where each coil image is stacked. Once coil sensitivity having complex values at each corresponding position of pixels is known, $\vec{\rho}$ value can be obtained by calculating the inverse of the matrix S [12].

$$\vec{\rho} = \widehat{(S^H \hat{S})^{-1}} \ \widehat{(S^H \cdot \vec{I})} \quad (4)$$

By solving the Eq. (4) repeatedly for each pixel in sensitivity encoding, and the full FOV reconstructed image is obtained [12].

Reference sequence of 3D FFE was consisted of NEX values of 2, 4, 6, 8, 10 and 12, repetition time (TR)/echo time (TE) 4.0/0.79 ms, FOV F-H 450 mm, R-L 300 mm, Thickness 3 mm over contiguous and Pix/Vox 4.69/4.69/3.00. T2 TSE sequence used for exams achieved SENSE factors of 1.2, 1.5, 1.8, 2.0, 2.2, 2.5, 2.8, 3.0, 3.2, 3.5, 3.8 and 4.0 at TR/TE 3000/100 ms, FOV F-H 256 mm, R-L256 mm, Thick 5 mm and Pix/Vox 0.46/0.46/5.00. Exams were conducted five times for each SENSE factor to measure signal intensity for the object, the posterior phase-encode direction and frequency direction. And SNR was calculated using mean values (Fig. 1). As shown in the Eq. (5), SNR was calculated by finding the difference in signal intensity between the area of the object and the background.

$$\text{SNR} = \frac{\text{SI of object}}{\text{SDN}} \quad (5)$$

SNR: signal to noise ratio
SDN: standard deviation of noise in the background
SI: signal intensity

And artifacts were measured as background signal intensity in the phase-encode direction (Fig. 2). The increase in SNR with two different NEX variations was

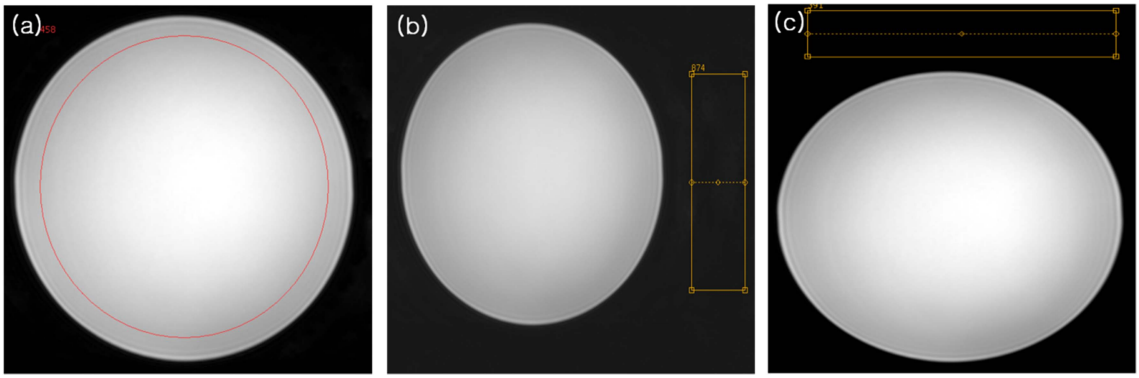

Fig. 1. (Color online) (a) Signal intensity was measured for the object, (b) the posterior phase direction and (c) frequency direction.

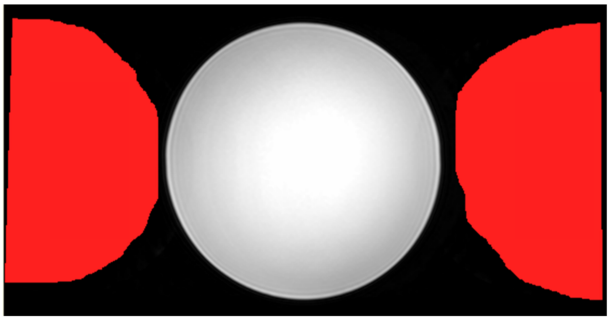

Fig. 2. (Color online) Artifacts were measured as background signal intensity in the phase-encode direction.

also investigated.

ANOVA (SPSS win 17.0 software, Chicago, USA) was used to determine the difference in mean vales between SNR in regions of interest obtained from three sense factors and background signal intensity in the phase direction. And Dunnett was used for post-hoc analysis. P values of less than 0.05 are considered statistically significant.

3. Results

3.1. SNR comparison between SESE factor and NEX

With 2 NEX, the highest SNR was 133.94 ± 21.32 at SENSE factor of 3.2 while the lowest SNR was 65.18 ± 10.45 at SENSE factor of 2 ($p < 0.05$). With 4 NEX, the highest SNR was 291.89 ± 24.65 at SENSE factor of 3.5 and the lowest SNR was 168.69 ± 17.85 at SENSE factor of 2.2 ($p < 0.05$). With 6 NEX, the highest SNR was 271.23 ± 26.35 at SENSE factor of 3.2 and the lowest SNR was 144.71 ± 15.32 at SENSE factor of 2.2 ($p < 0.05$). With 8 NEX, the highest SNR was 417.32 ± 35.65 at SENSE factor of 3.2 while the lowest SNR was 214.06 ± 20.13 at SENSE factor of 2.2 ($p < 0.05$). With 10 NEX, the highest SNR was 393.54 ± 36.32 at SENSE factor of 3.2 and the lowest SNR was 207.27 ± 25.62 at SENSE factor of 2.2 ($p < 0.05$). With 12 NEX, the highest SNR was 434.07 ± 39.21 at SENSE factor of 3.2 and the lowest SNR was 243.10 ± 25.62 at SENSE factor of 2.2 ($p < 0.05$).

In SNR comparison by SENSE factor, at factor of 1.2 the highest SNR was 304.91±23.52 with 12 NEX. At 1.5, the highest SNR was 285.37±28.52 with 8 NEX. At 1.8, the highest SNR was 281.32±16.32 with 12 NEX. At 2.0, the highest SNR was 243.10±32.12 with 12 NEX, At 2.2, the highest SNR was 243.10±25.62 with 12 NEX. At 2.5, the highest SNR was 360.40 ± 23.24 with 12 NEX, At 2.8, the highest SNR was 395.74 ± 35.55 with 12 NEX. At 3.2, the highest SNR was 434.07 ± 39.21 with 12 NEX. At 3.5, the highest SNR was 420.86 ± 40.20 with 12 NEX. At 3.8, the highest SNR was 430.97 ± 41.22 with 12 NEX. At 4.0, the highest SNR was 426.26 ± 36.98 with 12 NEX ($p < 0.05$) (Table 1) (Fig. 3). While there was no specific correlation between SNR and NEX variations, SNR increased with NEX 4, 8 and 12 showing

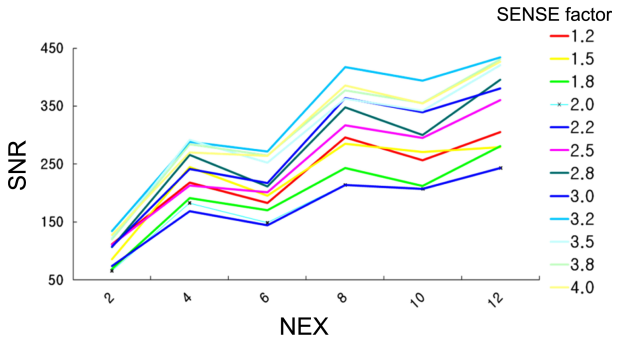

Fig. 3. (Color online) A graph showing changes in SNR resulting from NEX variations: SNR increased with NEX 4, 8 and 12 showing a M-shaped curve.

Table 1. SNR comparison between SENSE factor and NEX.

SENSE factor	2 NEX	P	4 NEX	P	6 NEX	P	8 NEX	P	10 NEX	P	12 NEX	P
1.2	111.58±23.20		217.90±25.65		182.84±19.35		295.85±29.65		256.46±16.23		304.91±23.52	
1.5	85.59±10.35		245.01±26.65		195.79±14.56		285.37±28.52		271.02±17.85		279.44±32.21	
1.8	69.28±12.36		191.24±19.69		170.46±17.98		242.79±27.65		212.54±20.31		281.32±16.32	
2.0	65.18±10.45		182.72±19.20		148.71±19.65		214.06±24.32		207.27±22.21		243.10±32.12	
2.2	73.79±12.65		168.69±17.85		144.71±15.32		214.06±20.13		207.27±21.45		243.10±25.62	
2.5	111.14±10.69	0.045	212.62±20.14	0.040	201.24±18.23	0.032	316.74±36.25	0.04	294.92±26.69	0.035	360.40±23.24	0.045
2.8	106.21±18.32		265.53±21.35		211.62±19.30		347.98±32.12		300.03±29.32		395.74±35.55	
3.0	107.05±19.03		241.33±22.37		217.06±21.65		363.71±30.24		339.56±32.21		380.32±36.62	
3.2	133.94±21.32		288.71±23.54		271.23±26.35		417.32±35.65		393.54±36.32		434.07±39.21	
3.5	122.64±22.30		291.89±24.65		252.27±27.22		362.81±34.21		341.76±37.25		420.86±40.20	
3.8	120.42±19.57		284.32±23.20		265.08±26.33		377.56±31.22		355.5±34.21		430.97±41.22	
4.0	127.89±17.69		269.72±24.35		263.85±21.74		385.52±39.24		361.45±33.21		426.26±36.98	

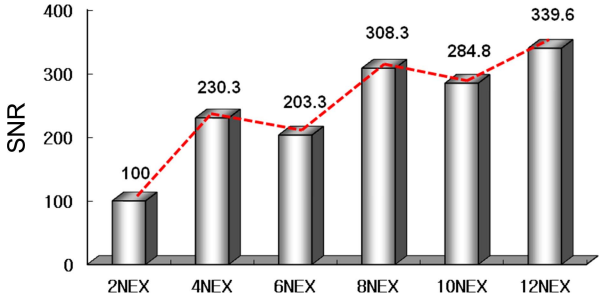

Fig. 4. (Color online) A graph showing increase in SNR with 2 NEX: SNR also increased with 2 NEX showing a M-shaped curve.

a M-shaped curve. SNR also increased on the basis of 2 NEX showing a M-shaped curve (Fig. 4).

3.2. SENSE artifacts comparison between SENSE factor and NEX

With 2 NEX, the highest SNR was 27.71 ± 2.35 at SENSE factor of 2.0 while the lowest SNR was 13.36 ± 1.25 at SENSE factor of 1.2 ($p < 0.05$). With 4 NEX, the highest SNR was11.78 ± 1.24 at 1.8 and the lowest SNR was 6.93 ± 0.65 at 4.0 ($p < 0.05$). With 6 NEX, the highest SNR was 14.79 ± 1.52 at 2.0 and the lowest SNR was 9.39 ± 1.39 at 4.0 ($p < 0.05$). With 8 NEX, the highest SNR was 9.02 ± 0.74 at 2.0 and the lowest SNR was 5.80 ± 0.44 at 3.2 ($p < 0.05$). With 10 NEX, the highest SNR was 9.12 ± 1.09 at 1.8 and the lowest SNR was 5.51 ± 0.61 at 4.0 ($p < 0.05$). With 12 NEX, the highest SNR was 8.03 ± 0.65 at SENSE factor of 1.5 and the lowest SNR was 4.70 ± 0.34 at SENSE factor of 4.0 ($p < 0.05$).

In changes in SNR with sense factors, a higher SNR was observed with 2 NEX at all SENSE factors ($p < 0.05$) (Table 2) (Fig. 5). There was no specific correlation between NEX variations and SNR. However, the graph

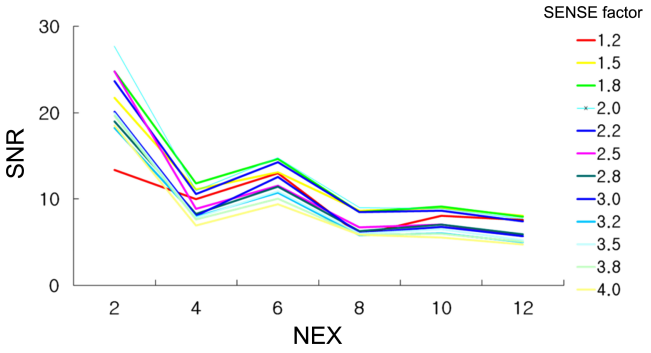

Fig. 5. (Color online) A SENSE artifact graph: Background SNR decreased with NEX of 4, 8 and 12 showing a W-shaped curve in artifact graphs.

Table 2. SENSE artifacts comparison between SENSE factor and NEX.

SENSE factor	2 NEX	P	4 NEX	P	6 NEX	P	8 NEX	P	10 NEX	P	12 NEX	P
T2 TSE SENSE 1.5	21.72±2.36		11.1±0.98		13.08±1.32		8.62±0.45		8.98±1.05		8.03±0.65	
T2 TSE SENSE 1.8	24.81±2.22		11.78±1.24		14.48±1.44		8.46±0.44		9.12±1.09		7.93±0.81	
T2 TSE SENSE 2.0	27.71±2.35		10.98±1.33		14.79±1.52		9.02±0.74		8.89±1.22		7.68±0.87	
T2 TSE SENSE 2.2	23.68±2.62		10.55±1.36		14.29±1.36		8.48±0.82		8.63±0.99		7.43±0.54	
T2 TSE SENSE 2.5	24.81±2.21		8.88±0.89		11.53±2.01		6.72±0.51		7.01±0.63		5.68±0.98	
T2 TSE SENSE 2.8	18.99±1.98	0.025	8.25±0.78	0.040	11.41±1.20	0.020	6.26±0.65	0.045	7.04±0.60	0.020	5.93±0.67	0.045
T2 TSE SENSE 3.0	20.11±2.03		8.07±0.89		12.54±1.47		6.06±0.66		6.75±0.44		5.71±0.72	
T2 TSE SENSE 3.2	18.25±2.11		7.97±0.92		10.71±1.54		5.80±0.44		6.01±0.71		5.02±0.43	
T2 TSE SENSE 3.5	19.97±1.99		7.86±0.94		10.90±1.28		6.04±0.49		6.49±0.65		5.19±0.39	
T2 TSE SENSE 3.8	19.65±2.01		7.64±0.88		10.03±1.34		5.85±0.37		5.98±0.44		5.04±0.41	
T2 TSE SENSE 4.0	18.49±1.89		6.93±0.65		9.39±1.39		5.84		5.51±0.61		4.70±0.34	

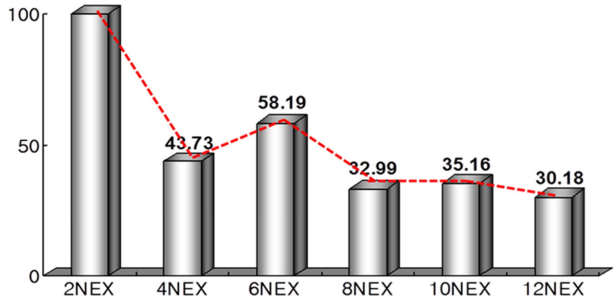

Fig. 6. (Color online) A graph showing increase in SNR with 2 NEX: SNR also increased with 2 NEX showing a M-shaped curve.

showing the relationship between SENSE artifacts and NEX variations, background signal intensity reduced with NEX 8 and 12 showing a W-shaped curve. SNR also increased on the basis of 2 NEX showing a M-shaped curve (Fig. 6).

4. Discussion

The use of parallel imaging of MRI has rapidly increased as means of fast imaging technique over the last decade. Parallel imaging is designed to obtain images simultaneously using multiple receive coils [13-16]. Two independent receive coils are placed to the object, and each coil is deemed to have sensitivity map in a rectangular shape (boxcar) and cover only half of the full FOV [13]. In other words, one receive coil detects signals from half of the object while the other coil detects signals from the other half. Separately, it is assumed that phase encoding steps should be taken N times to obtain data from the full FOV with balanced coil sensitivity [13]. However, data received by each coil after phase encoding steps for N times covers only half of the object based on the rectangular-shaped sensitivity map. This is described in Fig. 7. It is possible to reduce phase-encoding steps by half by adjusting the nature of coils. That is, using two receive coils designed to cover half of the full FOV simultaneously, phase-encoding steps need to be taken N/2 times not N times. And image acquisition time reduces as a result [13]. Accurate information on coil sensitivity map is required for accurate image reconstruction from sensitivity encoded data. A reference scan was therefore performed to obtain additional information on coil sensitivity before image reconstruction Reference scans do not provide information on absolute coil sensitivity. However, coil sensitivity map can be estimated by spatial scales used for image reconstruction under the assumption that each coil has the same spatial scale. A reference scan is therefore performed before the parallel imaging reconstruction. Despite the impact of reference on image reconstruction and quality, there has been few related studies of reference scans. This study was aimed to investigate effects of changes in SENSE factors and NEX on SNR and SENSE artifacts. While there was no specific correlation between SNR and NEX variations, SNR increased with NEX 4, 8 and 12 showing a M-shaped curve. SNR also increased with 2 NEX showing a M-shaped curve. There was no specific correlation between NEX variations and SNR. However, the graph showing the relationship between artifacts and NEX variations, background SNR decreased with NEX 8 and 12 showing a W-shaped curve. SNR also increased with 2 NEX showing a M-shaped curve. Generally, NEX increases SNR. But SNR showed a M-shaped curve in responses to changes in NEX in this study. It was reported that there can be additional loss of SNR depending on array layout of coils during sensitivity encoding in parallel imaging. In general, the coding efficiency at each position in FOV created by array layout of coils is expressed by a geometric factor. It is therefore claimed that SNR of completely reconstructed image is affected in sensitivity-encoding by g-factor as indicated by the following equation:

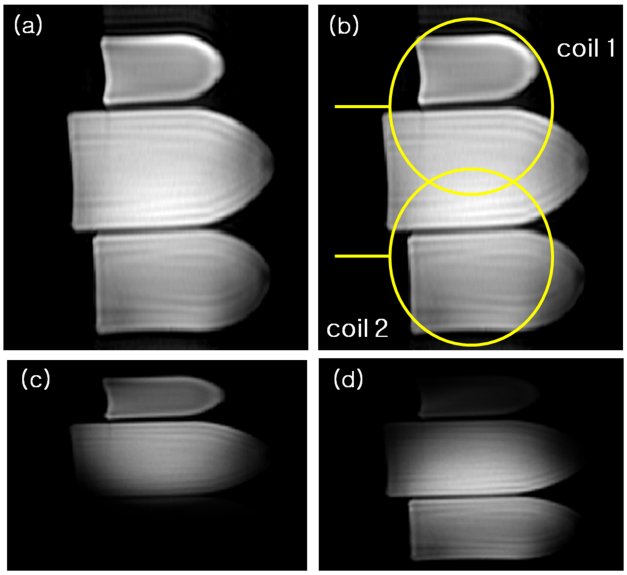

Fig. 7. (Color online) Diagram on the basic principles of parallel imaging techniques. (a) The full FOV images reconstructed through phase-encoding for N times (b) Layout of two coils having a rectangular-shaped sensitivity map (c) Reconstructed image from the first receive coil after phase-encoding for N times (d) Reconstructed image from the second receive coil after phase-encoding for N times.

$$\mathrm{SNR}_{\mathrm{SENSE}} = \frac{\mathrm{SNR}_{\mathrm{full}}}{\sqrt{\mathrm{R}} \cdot g} \tag{6}$$

This means that SNR can be also changed by a geo-

metry factor, which distorts the relationship between NEX variations and SNR. That is why SNR exhibited a M-shaped curve as NEX increased in this study, A geometry factor was likely to have an impact on the relationship between SENSE factors and SNR as well. Park *et al.* [17] measured effects on SNR resulted from each SENSE factor in three-dimensional MRI images. According to them, there was no significant difference in SNR with SENSE factors 2 and 3. But SNR increased with factor of 5. In this study, SENSE factors were more segmented and changes in SNR were measured. SNR decreased and subsequently increased in this study. On the contrary, background SNR increased and decreased as the effects of artifacts in sensitivity encoding. The decrease in background SNR was likely attributed to reduced noise in response to increasing SNR.

In conclusion, an increase in SNR and a decrease in artifacts were observed with NEX of 4, 8 and 12 when NEX increased in the reference scan performed using 8 channel head coils.

5. Conclusion

This study was conducted to identify how changes in NEX and SENSE factors affect image quality in a reference scan performed as a part of parallel imaging technique. SNR increased but SENSE artifacts reduced with NEX of 4, 8 and 12 when NEX increased in reference scan. It is therefore concluded that image quality can be improved with NEX of 4, 8 and 12 for reference scanning. The results of this study can be used to improve diagnostic efficiency in clinical practices.

Acknowledgments

Yeong-Cheol Heo and Hae-Kag Lee equally contributed to this work “This work was supported in part by the Soonchunhyang university Research Fund”.

References

[1] C. B. Ahn, J. H. Kim, and Z. H. Cho, IEEE Trans. Med. Imag **5**, 1 (1986).
[2] B. A. Poser and D. G. Norris, MAGMA **20**, 11 (2007).
[3] P. Mansfield, J. Phys. C **10**, 155 (1977).
[4] C. H. Meyer, B. S. Hu, D. G. Nishimura, and A. Macovski, Magn. Reson. Med **28**, 202 (1992).
[5] J. Hennig, A. Naureth, and H. Friedburg, Magn. Reson. Imag **3**, 823 (1986).
[6] D. K. Sodickson and W. J. Manning, Magn. Reson. Med. **38**, 591 (1997).
[7] K. P. Pruessmann, M. Weiger, M. B. Scheidegger, and P. Boesiger, Magn. Reson. Med. **42**, 952 (1999).
[8] M. Blaimer, F. Breuer, M. Mueller, R. M. Heidemann, M. A. Griswold, and P. M. Jakob, Top. Magn. Reson. Imag. **15**, 223 (2004).
[9] S. K. Park, C. B. Ahn, D. G. Sim, and H. C. Park, J. Korean Soc. Magn. Reson. Med. **12**, 123 (2008).
[10] P. G. Batchelor, D. Atkinson, P. Irarrazaval, D. L. Hill, J. Hajnal, and D. Larkman, Magn. Reson. Med. **54**, 1273 (2005).
[11] C. L. Christine, C. R. Jack, R. C. Grimm, P. J. Rossman, J. P. Felmlee, R. L. Ehman, and S. J. Riederer, Magn. Reson. Med. **36**, 436 (1996).
[12] S. K. Park, Sensitivity Encoding (SENSE) for Parallel MRI. Master's Thesis, Kwangwoon University (2007).
[13] J. F. Glockner, H. H. Hu, D. W. Stanley, L. Angelos, and K. King, Radiographics **25**, 1279 (2005).
[14] M. Weiger, K. P. Pruessmann, and P. Boesiger, Magnetic Resonance in Medicine **43**, 177 (2000).
[15] D. K. Sodickson and W. J. Manning, Magnetic Resonance in Medicine **38**, 591 (1999).
[16] K. P. Pruessmann, M. Weiger, P. Börnert, and P. Boesiger, Magnetic Resonance in Medicine **46**, 638 (2001).
[17] M. H. Park, J. W. Lee, K. W. Lee, C. W. Ryu, and G. H. Jahng, J. Korean. Soc. Magn. Reson. Med. **13**, 161 (2009).